Abdominal Radiology

Published online: 29 December 2015

Abdom Radiol (2016) 41:2–9
DOI: 10.1007/s00261-015-0594-6

Diffusion-weighted magnetic resonance imaging in the depiction of gastric cancer: initial experience

Lei Tang,[1] Ying-Shi Sun,[1] Zi-Yu Li,[2] Kun Cao,[1] Xiao-Yan Zhang,[1] Xiao-Ting Li,[1] Jia-Fu Ji[2]

[1]Department of Radiology, Key Laboratory of Carcinogenesis and Translational Research (Ministry of Education), Peking University Cancer Hospital & Institute, No.52 Fu Cheng Road, Hai Dian District, Beijing 100142, China
[2]Department of Gastrointestinal Surgery, Key Laboratory of Carcinogenesis and Translational Research (Ministry of Education), Peking University Cancer Hospital & Institute, No.52 Fu Cheng Road, Hai Dian District, Beijing 100142, China

Abstract

The aim of the study was to explore the feasibility of diffusion-weighted magnetic resonance imaging (DW-MRI) in the depiction of gastric cancer and to investigate the signal characteristics and apparent diffusion coefficient (ADC) of gastric cancer. An institutional review board-approved protocol was developed for this prospective study. DW-MRI was performed on 101 patients with gastric cancer that was detected by gastroscopy biopsy. The optimal number of excitations (NEX) for DW-MRI was determined, and the signal characteristics of gastric cancer on DW-MRI were analyzed. The ADC of gastric cancer was measured by two experienced radiologists independently, and the reproducibility of measurement was investigated by the Bland–Altman analysis. When DW-MRI was used with four NEXs, areas of gastric cancer showed a good contrast and contrast-to-noise ratio. Four kinds of signal characteristics of gastric cancer were observed on DW-MRI: uniformly high signal, inner high signal, and outer low signal (two-layer type), high–low–high signal (three-layer sandwich type), and mixed type. The mean ADC of gastric cancer measured by two observers was $(1.18 \pm 0.29) \times 10^{-3}$ mm^2/s and $(1.20 \pm 0.31) \times 10^{-3}$ mm^2/s respectively, which showed good agreement with Bland–Altman analysis (95% limits of agreement: -0.16 to $+0.19 \times 10^{-3}$ mm^2/s). Gastric cancers have various signal characteristics on DW-MRI and the reproducibility of ADC measurement is satisfactory. DW-MRI is helpful in the depiction of gastric cancer.

Correspondence to: Lei Tang; *email:* terrytang78@163.com

Key words: Stomach neoplasms—Diffusion-weighted imaging—Magnetic resonance imaging—Apparent diffusion coefficient—Reproducibility

Gastric cancer is one of the most common malignant tumors worldwide, with a high prevalence and mortality rate [1]. Early detection and comprehensive treatment are important for improving the prognosis of gastric cancer [2]. The conventional imaging techniques, such as fluoroscopic X-ray and computed tomography (CT), play an important role in the detection and evaluation of gastric cancer. However, these techniques have limitations because of the low soft-tissue contrast on X-ray-based imaging. Therefore, the tumor infiltration degree cannot be evaluated reliably [3]. Presently, magnetic resonance imaging (MRI) is being used for the diagnosis of gastric cancer [4, 5]. It yields better soft-tissue resolution than CT and can provide multiple sequences and contrasts to aid in the comprehensive evaluation of gastric cancer [4, 5].

Diffusion-weighted MRI (DW-MRI) is a non-invasive MRI technique. It employs a pair of motion-probing gradients to generate contrast which reflects the structural change in biological tissues at the microscopic level by indirectly monitoring the movement of water molecules [6–8]. DW-MRI was first used for the detection of early-stage ischemia and evaluation of intracranial tumors in the brain. With technical developments, body DW-MRI is being used as a new biomarker for the detection and therapeutic evaluation of neoplasms in abdominal organs [6–8]. Previous studies on abdominal organs had demonstrated the ability of DW-MRI to highlight tumor signals, such as those from liver, pan-

creas, kidney, and rectum [9–11]. The combination of DW-MRI with conventional MRI sequences can increase the detection rate and improve the depiction of tumors in abdominal organs [9–11].

DW-MRI of solid organs in the upper abdomen, such as the liver, spleen, and pancreas, is often influenced by macroscopic motion, and breath-hold is usually required to stabilize the organs during the imaging sequence [9, 10]. In the background of normal solid tissues, the signal-to-noise ratio (SNR) of DW-MRI with fewer numbers of excitations (NEX) allowable during one breath-hold is acceptable. With regard to DW-MRI of pelvic hollow viscera, such as the rectum [11] and uterus [12], which are free of respiratory influence and thus do not require breath-hold for imaging, an intrinsically low SNR becomes the main disadvantage, and multi-NEX is usually used to improve the SNR. However, DW-MRI of stomach is affected by both unfavorable factors of macroscopic motion and low SNR. Balancing NEX with breath-hold is a crucial problem in obtaining optimal DW-MRI images of gastric cancer. In this article, we investigate the feasibility and reproducibility of DW-MRI of gastric cancer through technical exploration in order to achieve high-quality DW-MRI for clinical applications.

Materials and methods

Patients and pre-examination

This prospective study was performed in accordance with the guidelines of the institutional ethical review board, and all the patients provided written informed consents. The inclusion criteria for the patients were (a) gastroscopy biopsy-proved gastric cancer, (b) able to tolerate breath-holding for at least 15 s, (c) no history of gastric operation, (d) no previous anticancer therapy, and (e) no contraindications for MR examination. A total of 105 consecutive patients who met the entry criteria were scanned using MRI.

The exclusion criteria were (a) cannot tolerate the complete MR examination process (1 patients were excluded) and (b) severe distortion of the images that influenced the stable measurement of the quantitative parameters (3 patients were excluded).

Finally, 101 patients (77 males and 24 females; mean age 63 years; age range 34–83 years) met the above criteria and were enrolled in this study.

The gastric cancers were found to be located in the cardia and fundus ($n = 38$), body ($n = 21$), antrum ($n = 40$), and the whole stomach ($n = 2$). There were 63 patients who accepted radical excision, while the remaining 38 patients were treated by palliative chemotherapy. There were eight cases of early gastric cancer (EGC) and 93 cases of advanced gastric cancer (AGC).

All the patients underwent MR examination on empty stomach after fasting overnight. If no contraindications (e.g., glaucoma, prostate hypertrophy, asthma, or severe heart diseases) were present, the patients were given 20 mg of scopolamine intramuscularly. After 10 min, they were orally administered tap water (800–1000 mL) to distend the gastric lumen. Then the patients lay on the examination bed supinely.

Routine MR imaging

An MR examination was performed using a 1.5-T scanner (GE Signa 1.5T EchoSpeed Plus with EXCITE II) with a maximum gradient strength of 33 mT/m and a slew rate of 120 mT/(m/ms). An eight-channel body phase-array coil and parallel imaging with an acceleration factor of two were used.

Prior to DW-MRI, all the patients were examined under the routine gastric MR protocols to localize the tumors and provide morphologic details. The sequences included T1-weighted fast spoiled gradient sequence (FSPGR; repetition time/echo time 150–200/4.2 ms; flip angle 80°; matrix size 320 × 160; section thickness 5 mm; section gap 1 mm; field of view 36–40 cm; NEX 1) and T2-weighted fast-recovery fast spin-echo sequence (FRFSE; repetition time/echo time 2 respiratory intervals/85 ms; matrix size 320 × 224; section thickness 5 mm; section gap 1 mm; field of view 36–40 cm; NEX 4; respiratory triggering). If the cancer signals were blurred by macromovement on respiratory triggering T2 images, a breath-hold T2-weighted single-shot fast spin-echo sequence (SSFSE: repetition time/echo time 2000/90 ms; matrix size 384 × 256; section thickness 5 mm; section gap 1 mm; field of view 36–40 cm; number of excitation 0.57) was taken as a substitute.

Diffusion-weighted MR imaging

DW-MRI was performed using a single-shot echo-planar imaging sequence (SS-EPI) in the transverse plane during breath-hold. The patients were divided into two groups. In the first group, the optimum balance between the NEX and breath-hold was investigated. In the second group, diffusion signal characteristics of cancers, reproducibility of apparent diffusion coefficient (ADC) measurements, and detection ability were further explored.

Group 1

A total of initial 32 consecutive patients were enrolled in this group, and each patient was imaged using three diffusion-weighted sequences with different NEXs. The sequences used were as follows: (1) sequence 1, 1 NEX, imaging time 10 s; (2) sequence 2, 2 NEXs, imaging time 21 s; and (3) sequence 3, 4 NEXs, imaging time 41 s. The other parameters were the same for three sequences: repetition time/echo time 2750/65 ms; field of view 40 cm; matrix 128 × 128; section thickness 5 mm;

intersection gap 1 mm. The pulses generated using the manual pulse generator (MPG) were placed in three directions (x-, y-, and z-axes), and the b-factors were 0 and 1000 s/mm^2. If the imaging time exceeded the patient's breath-hold endurance, the sequence was segmented into several breath-holds using a pause scan function key [6].

Group 2

A total of 69 consecutive patients enrolled in this group. All the patients underwent a DW-MRI examination with the optimum NEXs as defined in Group 1.

Image analysis

All MR images were analyzed on a GE AW 4.2 workstation using the Functool 2 software. Two experienced radiologists (L.T. and K.C., with 12 and 13 years of experience in clinical MRI, respectively) who knew the results of the endoscopic biopsy evaluated the data.

(1) Placement of region of interest (ROI)

The image slice containing the largest area of cancer was chosen on DW-MRI, and a curved line was drawn by free hand to include the high cancer signal as ROI. The size of the ROI was no less than 20 mm^2. The signal intensity of cancer (S_{Ca}, mean ± SD) was recorded. In addition, an ROI was placed on adjacent normal gastric wall area, and the signal intensity was recorded (S_{wall}, mean ± SD). If normal gastric wall was not visible on DW-MRI, then the $b = 0$ s/mm^2 images were taken as reference.

(2) Image quality evaluation

The two radiologists evaluated the image quality of the three DW-MRI sequences in 32 cases according to the image quality scale and the contrast-to-noise ratio (CNR). The third radiologist (Y.S.S., with 15 years of experience in clinical MRI) made independent evaluations when any disagreement occurred.

Image quality scale (IQS). Grade I, no artifact (mainly as a parallel imaging reconstruction artifact) was demonstrated, and the background signal was even and had good cancer contrast; Grade II, slight artifacts were seen without affecting the display of cancer and the measurements of ADC; Grade III, conspicuous artifacts influenced the display of cancer and/or the measurements of ADC.

Contrast-to-noise ratio (CNR). We recorded the signal intensity of S_{Ca} and S_{wall} on ROI of DW-MRI, $\Delta S = S_{Ca} - S_{wall}$. Oval ROIs (with diameter > 2 cm) were placed on the anterior and posterior background (phase encoding direction), and the average was taken as the signal intensity of the background noise (S_{BN}). CNR was calculated by one radiologist (L.T.) using the formula: $CNR_{Ca\text{-}wall} = \Delta S/SD_{BN}$.

(3) Cancer detection and measurement of ADCs

The two radiologists independently evaluated whether gastric cancer could be detected on DW-MRI and whether the ADC of cancers could be measured in all the cases. The criteria included a distinguishable high signal of the cancer to nearby gastric wall and no obvious deformation and/or artifacts influencing ADC measurement on at least one slice. The ADC of gastric cancer was measured using a curved ROI to include the high signal. ADC was read out on ADC maps, each of which was measured twice, and the average was taken.

Statistical evaluation

Statistical analyses were performed using the statistical software SPSS (version 11.5). The IQS was compared using Fisher's exact test. A paired t test was used if the distribution was normal; otherwise, a Wilcoxon rank-sum test was used to compare the CNR of the different DW-MRI sequences. An interobserver agreement for cancer detection and ADC measurability between the two radiologists was evaluated using kappa statistics. A kappa value of >0.20 indicated poor agreement, value of 0.21–0.40 indicated fair agreement, value of 0.41–0.60 indicated moderate, value of 0.61–0.80 indicated good, and the value of 0.81–1.00 indicated excellent agreement. Interobserver coherence of ADCs measurement was determined by the Bland–Altman analysis to calculate the mean difference and 95% limits of agreement (LOA). A difference with $P < 0.05$ indicated statistical significance.

Results

Choice of NEXs for gastric cancer DW-MRI

In Group 1, all 32 lesions were detected on DW-MRI images as high signals, and the ADC could be reliably measured in 31 cases. The ADC could not be measured in one case due to severe image distortion caused by air-fluid level. With increasing NEX, the grade of IQS improved; there was a statistically significant difference between one NEX and four NEXs ($X^2 = 18.998$, $P < 0.01$), but no significant difference was found between one NEX and two NEXs ($X^2 = 4.582$, $P = 0.093$). On DW-MRI with four NEXs, all cancer cases had good contrast (Fig. 1). With increasing NEX, the $CNR_{Ca\text{-}wall}$ value increased, and there was a statistically significant difference between one NEX and two NEXs ($t = -7.220$, $P < 0.01$) and between one NEX and four NEXs ($t = -11.377$, $P < 0.01$) (Table 1).

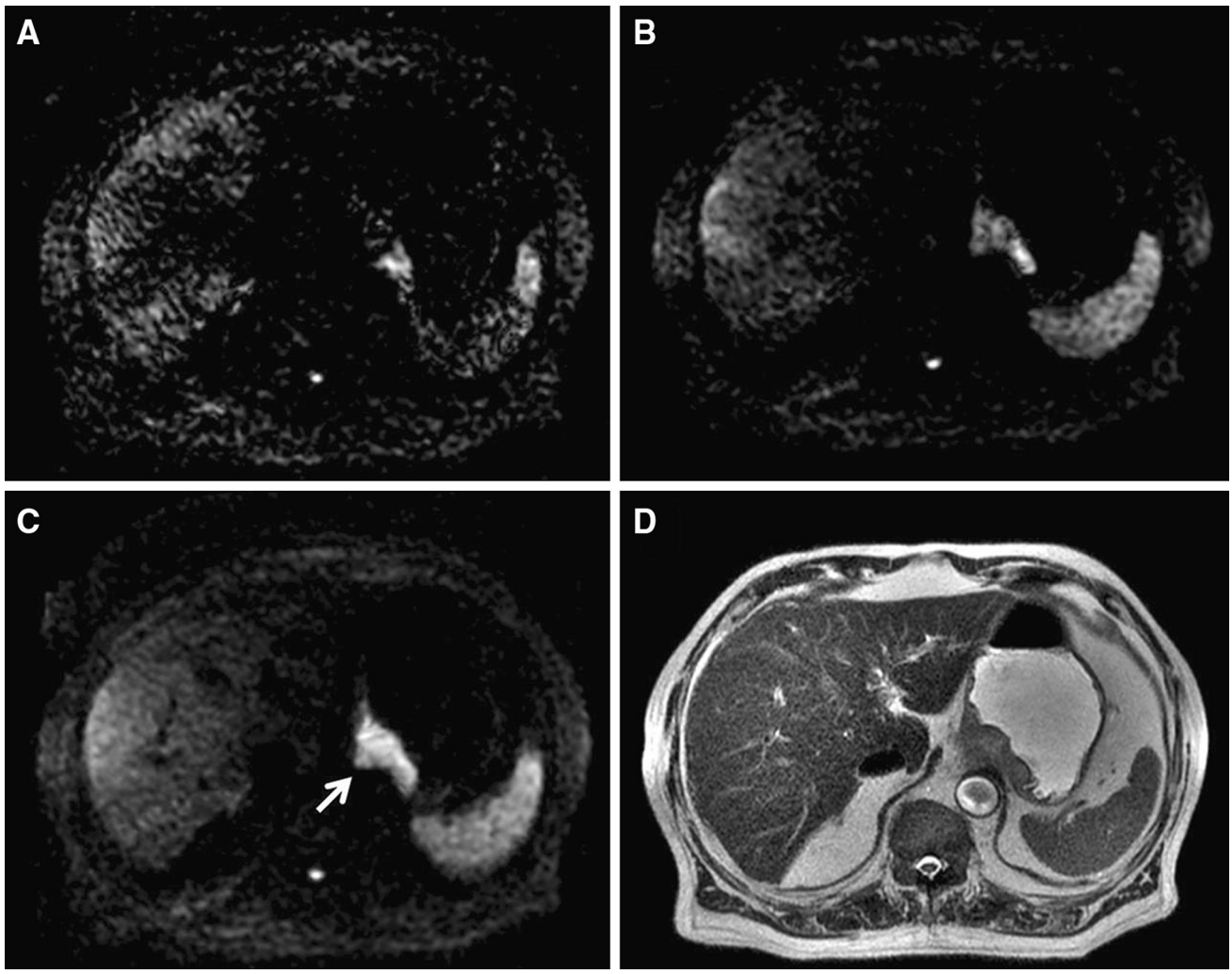

Fig. 1. Image quality of DW-MRI sequences with different NEXs. **a** One NEX. **b** Two NEXs. **c** DW-MRI with four NEXs. This showed more uniformity in tumor signals and fewer artifacts than (**a**) and (**b**). **d** Routine MR images of SSFSE.

Table 1. IQS and $CNR_{Ca\text{-}wall}$ for DW-MRI sequences with different NEXs

NEXs	IQS			$CNR_{Ca\text{-}wall}$
	I	II	III	
1	5	11	15	9.48 ± 4.76
2	9	15	7	15.17 ± 5.41
4	15	16	0	23.63 ± 7.84

Signal characteristics of gastric cancer on DW-MRI

Of the 101 cases, 100 cases were interpreted identically for cancer detection by the two radiologists, resulting in preferable coherence with a kappa value of 0.852 ($P < 0.01$). In 97 gastric cancer cases, the two observers agreed that the DW-MRI showed a high signal compared to the adjacent normal gastric wall. Three EGCs and one AGC (pT2) with length–diameter less than 3 cm (confirmed by operation) were not obviously depicted on DW-MRI, and these four cases were not detected on either T1-weighted images or T2-weighted images. The demonstration rate was 63% (5/8) for EGC and 99% (92/93) for AGC on DW-MRI.

Of the total, 49 cases (51%) displayed a uniformly high signal, while the remaining 48 cases (49%) displayed a non-uniformly high signal, which can be subdivided into three types: (1) two-layer type (inner high signal and outer low signal, 16 cases), (2) three-layer type (high–low–high sandwich signal, 12 cases), and (3) mixed type (scattered dot-like high signal, 20 cases) (Fig. 2).

Reproducibility of ADC measurements

A total of 98 cases were interpreted identically for ADC measurability by the two radiologists, resulting in preferable coherence with a kappa value of 0.826 ($P < 0.01$). In case of 90 gastric cancer cases (89%), the two observers agreed that ADCs could be measured. The mean ADCs for gastric cancer measured by the two

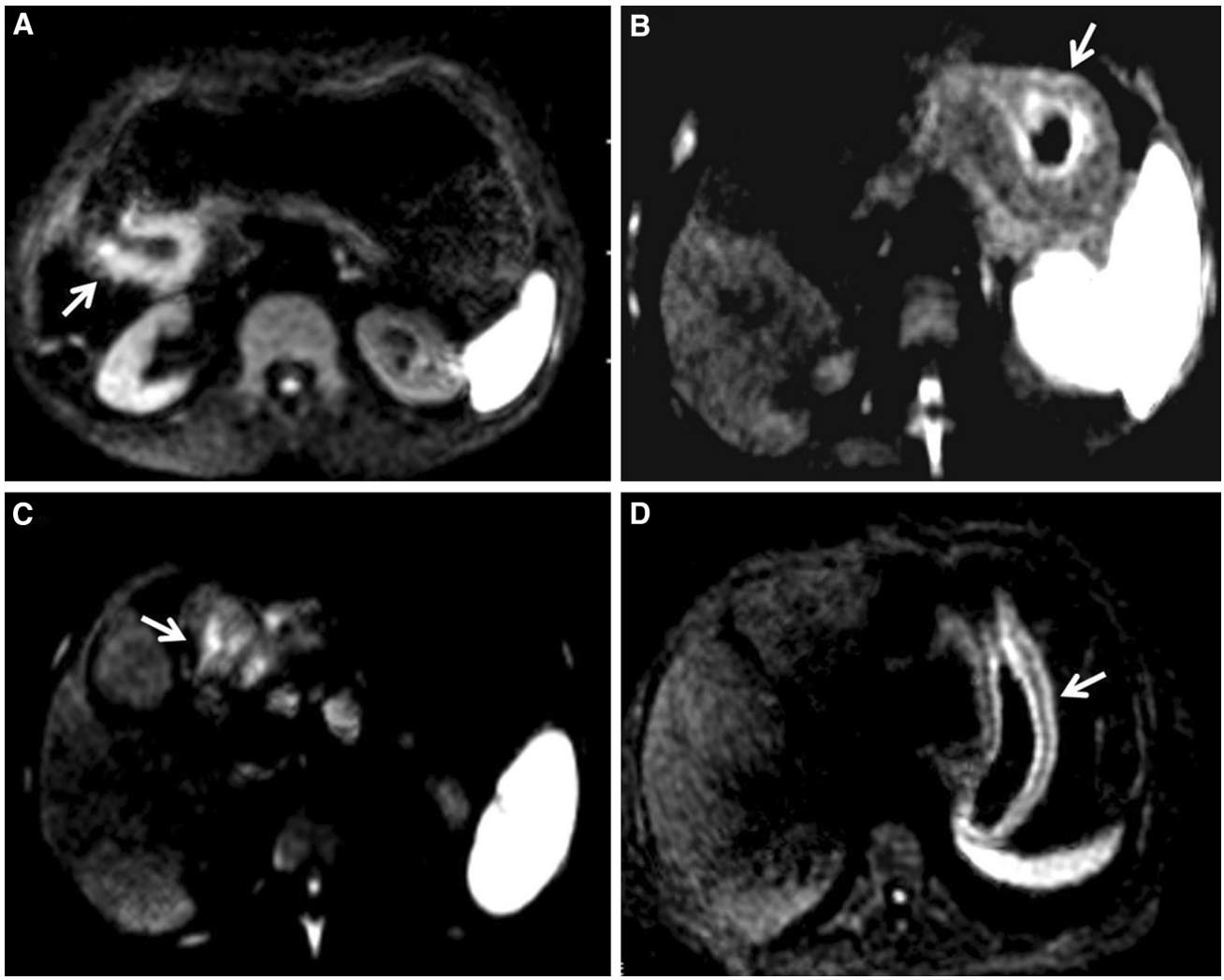

Fig. 2. Signal characteristics of gastric cancer on DW-MRI. **a** Uniformly high signal. **b** Two-layer type. **c** Mixed type. **d** Three-layer type ("Sandwich" sign).

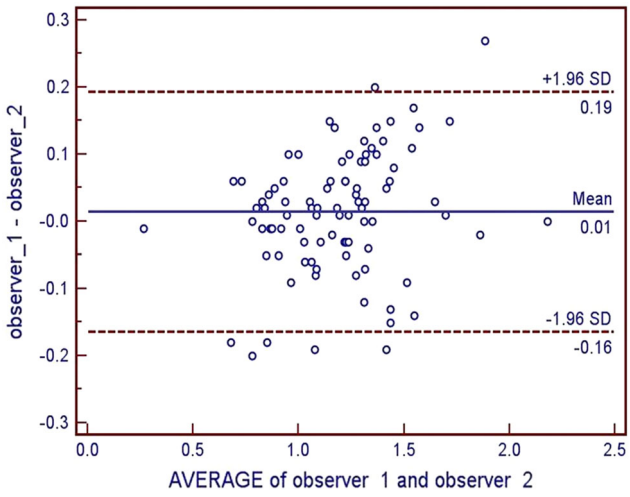

Fig. 3. Bland–Altman plot of the difference between ADC measurement for observers 1 and 2 against the mean measurement, with 95% LOA (both readers).

observers were $(1.18 \pm 0.29) \times 10^{-3}$ mm^2/s and $(1.20 \pm 0.31) \times 10^{-3}$ mm^2/s, respectively, which shows a good correlation ($r = 0.957$, $P < 0.001$).

The Bland–Altman analysis further showed a good agreement between the two radiologists for ADC measurement (Fig. 3). The mean difference in ADC measurement between the two observers was 0.01×10^{-3} mm^2/s (95% LOA: -0.164 to $+0.194 \times 10^{-3}$ mm^2/s). The average of the differences was 0.0148, which was approximately 1% of the average of two observers. The SD of the differences was 0.091. Ninety scatters were found to be around the bias line with no trend as the average varied, and seven (7.8%) were outside of 95% LOA. The figure indicated good reproducibility of measured ADC between the two observers to be around 0.2–2.2 cm.

Discussion

DW-MRI is a non-invasive technique capable of probing structural changes in biologic tissues at a microscopic

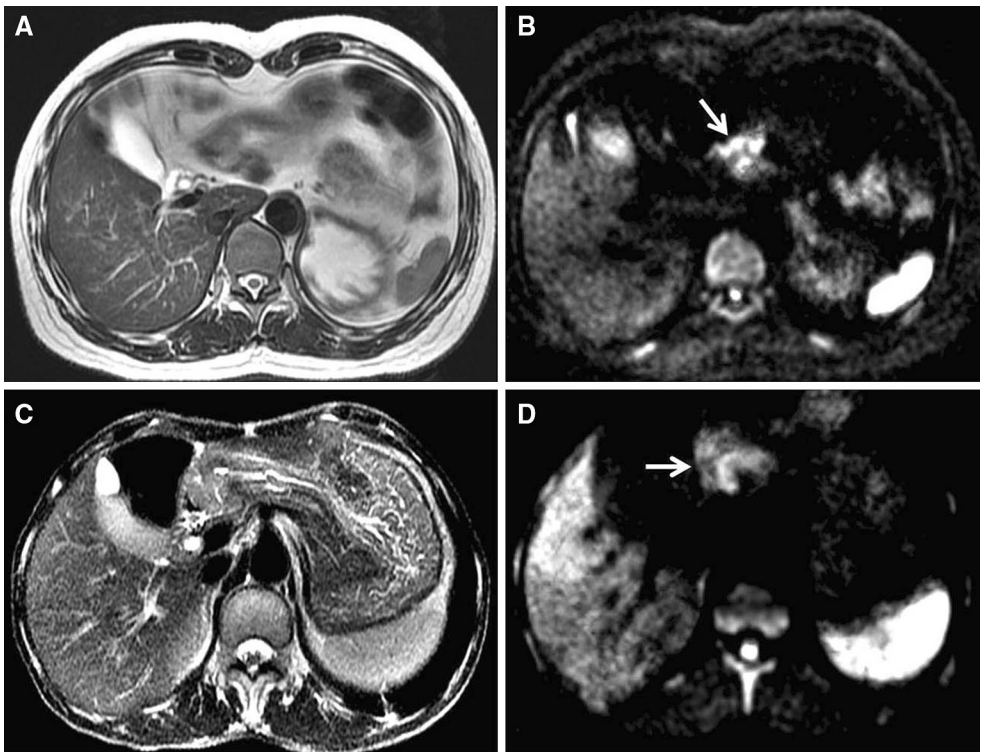

Fig. 4. Cancer detection of non-enhanced MRI combined with DW-MRI (**a**) FRFSE T2WI, the cancer signal was blurred because of gastric peristalsis. **b** FRFSE T2WI, the cancer appeared as a high signal on DW-MRI (*white arrow*). **c** SSFSE T2WI, the cancer signal was hard to detect because of less fat space around the stomach. **d** SSFSE T2WI, the cancer appeared as a high signal on DW-MRI (*white arrow*).

level [6–12]. It provides a new contrast for tumor detection, diagnosis, and therapeutic response evaluation through the variation of water molecules diffusion between the tumor and nearby normal tissues. With increase in technical developments, more studies are focusing on body DW-MRI imaging. It has been verified that DW-MRI is helpful in the detection of tumors in various abdominal organs such as the liver [10], pancreas [9], rectum [11], and uterus [12]. Furthermore, the ADC calculated from DW-MRI signals provides a new surrogate biomarker for therapeutic effect evaluation of neoplasms [13].

The main challenge in the imaging of abdominal DW-MRI lies in the contradiction between the breath-hold technique to inhibit respiratory motion and the multi-NEX to improve the SNR. Breath-hold restricts imaging time, which results in fewer acquisitions and thus in poor SNR. Therefore, there are usually two sets of imaging protocols for abdominal DW-MRI. In the solid organs of the upper abdomen, breath-hold is used, and SNR with one to two NEXs during one breath-hold (imaging time: 15–20 s) is acceptable due to the relatively even background signal [9, 10]. However, in the pelvic hollow viscera (e.g., rectum and uterus), intrinsically low SNR becomes the primary disadvantage, and breath-hold is not necessary as the influence of respiratory movements is slight; therefore, usually six to eight NEXs (imaging time: 2–3 min) are taken for optimal SNR [14].

In the case of the stomach, which is located in the upper abdomen, breath-hold should be used as the respiratory movement influences DW-MRI and ADC measurement. Moreover, as the stomach is a hollow visceral organ with intrinsically low SNR on DW-MRI, multi-NEXs should also be used, but the time necessary for this is not permitted by breath-hold. Thus, determining how to balance multi-NEX and breath-hold becomes a critical problem.

In this study, we explored a combined method for obtaining optimal gastric DW-MRI data. First, the so-called segmented breath-hold method was used to resolve the conflict between short breath-hold time and time-consuming multi-NEX acquisition. If the imaging time exceeded a patient's breath-hold endurance, then the diffusion-weighted sequences were segmented into several breath-holds using a "pause scan" function, which was previously used [6].

On this basis, we explored the lower limit of NEXs to achieve acceptable DW-MRI data for gastric cancer. We found that the image quality was better with four NEXs, for which all cancer cases showed good contrast and no artifacts influenced the display of cancer and measurement of ADCs. Under these conditions, the imaging time

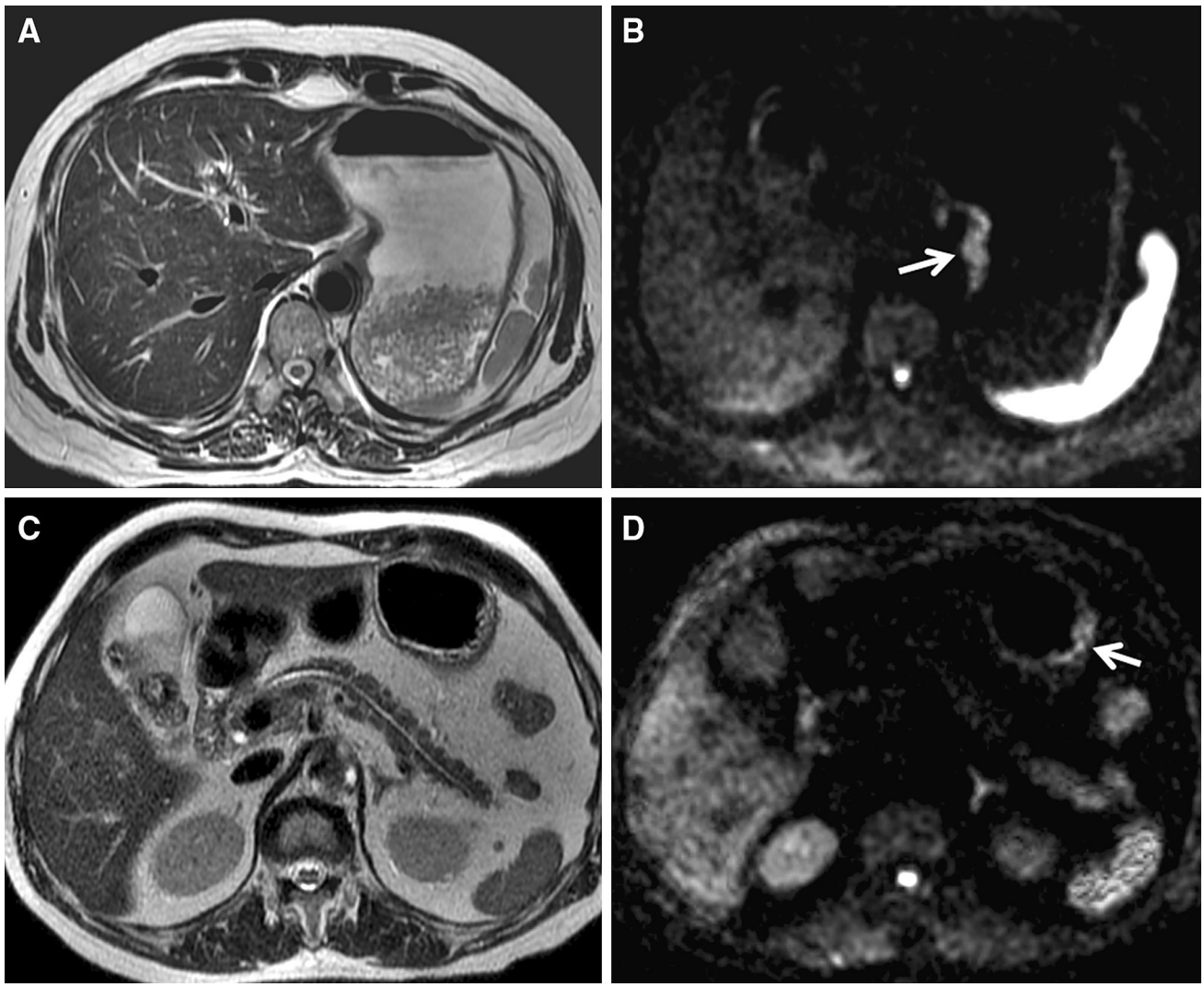

Fig. 5. Cancer detection of non-enhanced MRI combined with DW-MRI (**a**) FRFSE T2WI, the cardiac wall displayed a thickness of the gastric wall <8 mm and no detectable thickness difference compared to nearby normal gastric wall and without a signal difference. **b** FRFSE T2WI, the cancer appeared as a high signal on DW-MRI (*white arrow*). **c** SSFSE T2WI, the wall of gastric body displayed a thickness of the gastric wall <8 mm and no detectable thickness difference compared to nearby normal gastric wall and without a signal difference. **d** SSFSE T2WI, the cancer appeared as a high signal on DW-MRI (*white arrow*).

was 41 s, and the patients could use two breath-holds to complete the entire examination. Therefore, this approach was recommended as a routine parameter for high *b* value DW-MRI of gastric cancer.

The signal characteristics of gastric cancer on DW-MRI were also evaluated. In total, 97 of the 101 cases of gastric cancer showed a high signal on DW-MRI compared to adjacent normal gastric wall. Further investigation concluded that gastric cancer showed different signal characteristics on DW-MRI. Half of the cases showed a uniformly high signal, while the other half displayed a non-uniform signal, which could be further subdivided into three types: a two-layer type (inner high signal, outer low signal), a three-layer type (high–low–high signal appearing as a ''sandwich'' sign), and a mixed type (scattered dot-like high signal). The clinical significance of these different signal characteristics needs further research.

Investigation of the reproducibility of ADC measurements is an important step prior to its clinical use [15, 16]. In this study, two observers obtained preferable coherence for gastric cancer detection and ADC measurability judgment, resulting in kappa values of 0.852 and 0.826. The ADCs measured by the two observers also showed good correlation. The Bland–Altman analysis further showed good agreement between the two observers for ADC measurement, with a mean difference in ADC values between the two observers being only 0.0148×10^{-3} mm^2/s, and only seven values (7.8%) are outside of 95% LOA.

Finally, we investigated the preliminary clinical application of DW-MRI, mainly focusing on its additional value in cancer description. Previous studies with abdominal organs have demonstrated the ability of DW-MRI to highlight tumor signals such as those in the liver, pancreases, kidney, and rectum [8–12]. In our study, the depiction of gastric cancer was also highlighted by DW-MRI. This improvement may be attributed to the high cancer signal contrast provided by DW-MRI, which can highlight cancer signals while depress signals from nearby normal tissues. This is especially helpful in the following three conditions:

(1) In patients with poor hypotonic performance, the artifacts produced by gastric peristalsis blur the cancer signal upon respiratory triggering fast spin echo (FSE), and supplementary DW-MRI can help in the depiction of the cancer location and border (Fig. 4a, b).
(2) In emaciated patients with less abdominal fat, the cancer signal on conventional T1WI and T2WI may be hard to be discriminated from nearby normal tissues. This can be highlighted by DW-MRI through the depression of normal tissue signals (Fig. 4c, d).
(3) In those small lesions, which lack both morphological and signal differences to nearby normal gastric wall, DW-MRI can help in highlighting cancer signals (Fig. 5).

There were several potential limitations in our study. First, because the thickness of the normal gastric wall is often smaller (3 mm) under full extension, it was hard to put ROI on the normal gastric wall to get objective and accurate ADCs. So we did not set control group. Second, as an experimental study, the MRI examination was performed as a supplement to enhanced CT, so most of our cases were not performed enhanced sequences, which may provide more information. Third, in order to declare that the four NEXs are the lowest-necessary NEXs, we should have demonstrated that the higher NEX does not significantly improve image quality of DW-MRI. However, considering the time-consuming acquisition of higher NEX, it would have produced heavy burden on the patients' breath-hold. So, after we got optimal images with 4 NEXs, a further increase of acquisition numbers was not performed. Fourth, the two observers knew the location of the cancers by endoscopic biopsy before evaluation, in order to facilitate the measurement of the cancer ADC; the defect of the above design was the influence to the subjective evaluation of the detective diversity by two observers. Further study need to clarify this aspect.

In conclusion, we used segmented breath-hold to resolve the contradiction between macro-motion and low SNR and found four NEXs to be the optimal acquisition time for DW-MRI of gastric cancer. The acquired images have high quality, and the reproducibility of cancer detection and ADC measurement is satisfied. DW-MRI is helpful in the depiction of gastric cancer. Finally, it should be emphasized that although DW-MRI can provide high tumor-to-normal tissue contrast of gastric cancer, the difficulty of localization caused by background signal depression cannot be ignored. It should not be used independently, but as a supplementary means to further improve the detection and depiction of gastric cancer.

Acknowledgments This work was supported by the National Natural Science Foundation of China (Grant Nos. 81201215, 81371715) and Natural Science Foundation of Beijing (Grant No. 7132039).

Compliance with ethical standards

Conflict of interest The authors declare no conflict of interest.

References

1. Torre LA, Bray F, Siegel RL, et al. (2015) Global cancer statistics, 2012. CA Cancer J Clin 65:87–108
2. Hajj C, Goodman KA (2015) Role of radiotherapy and newer techniques in the treatment of GI cancers. J Clin Oncol 33:1737–1744
3. Seevaratnam R, Cardoso R, McGregor C, et al. (2012) How useful is preoperative imaging for tumor, node, metastasis (TNM) staging of gastric cancer? A meta-analysis. Gastric Cancer 15:S3–S18
4. Joo I, Lee JM, Han JK, et al. (2015) Dynamic contrast-enhanced MRI of gastric cancer: correlation of the perfusion parameters with pathological prognostic factors. J Magn Reson Imaging 41:1608–1614
5. Lei C, Huang L, Wang Y, Huang Y, Huang Y (2013) Comparison of MRI and endoscope ultrasound detection in preoperative T/N staging of gastric cancer. Mol Clin Oncol 1:699–702
6. Zhang XP, Tang L, Sun YS, et al. (2012) Sandwich sign of Borrmann type 4 gastric cancer on diffusion-weighted magnetic resonance imaging. Eur J Radiol 81:2481–2486
7. Sheng RF, Zeng MS, Ji Y, et al. (2015) MR features of small hepatocellular carcinoma in normal, fibrotic, and cirrhotic livers: a comparative study. Abdom Imaging 40(2015):3062–3069
8. Liu S, Guan W, Wang H, et al. (2014) Apparent diffusion coefficient value of gastric cancer by diffusion-weighted imaging: correlations with the histological differentiation and Lauren classification. Eur J Radiol 83:2122–2128
9. Kim H, Arnoletti PJ, Christein J, et al. (2014) Pancreatic adenocarcinoma: a pilot study of quantitative perfusion and diffusion-weighted breath-hold magnetic resonance imaging. Abdom Imaging 39:744–752
10. Chen ZG, Xu L, Zhang SW, Huang Y, Pan RH (2015) Lesion discrimination with breath-hold hepatic diffusion-weighted imaging: a meta-analysis. World J Gastroenterol 21:1621–1627
11. Moreno CC, Sullivan PS, Kalb BT, et al. (2015) Magnetic resonance imaging of rectal cancer: staging and restaging evaluation. Abdom Imaging. 40(7):2613–2629
12. Jha RC, Zanello PA, Ascher SM, Rajan S (2014) Diffusion-weighted imaging (DWI) of adenomyosis and fibroids of the uterus. Abdom Imaging 39:562–569
13. Tang Lei, Zhang Xiao-Peng, Sun Ying-Shi, et al. (2011) Gastrointestinal stromal tumors treated with imatinib mesylate: apparent diffusion coefficient in the evaluation of therapy response in patients. Radiology 258:729–738
14. Sun YS, Zhang XP, Tang L, et al. (2010) Locally advanced rectal carcinoma treated with preoperative chemotherapy and radiation therapy: preliminary analysis of diffusion-weighted MR imaging for early detection of tumor histopathologic downstaging. Radiology 254:170–178
15. Klerkx WM, Mali WM, Peter Heintz A, et al. (2011) Observer variation of magnetic resonance imaging and diffusion weighted imaging in pelvic lymph node detection. Eur J Radiol 78:71–74
16. Kwee TC, Takahara T, Koh DM, Nievelstein RA, Luijten PR (2008) Comparison and reproducibility of ADC measurements in breathhold, respiratory triggered, and free-breathing diffusion-weighted MR imaging of the liver. J Magn Reson Imaging 28:1141–1148